

Hydrodynamics of Undulatory Fish Locomotion

Nicholas Taluzek,^{1,a,b)} Dr. Sharath Girimaji^{2,c)}

¹ *Department of Mechanical, Materials, and Aerospace Engineering, Illinois Institute of Technology, Chicago Illinois, 60616, USA*

² *Department of Aerospace Engineering, Texas A&M University, 77843, College Station, Texas, USA*

While fish utilize their complex musculature to propel themselves through water, simplifying the complex motions of fish locomotion into simpler mechanical systems will allow us to design more efficient propulsion devices for neutrally buoyant craft such as submarines and airships. In this study the hydrodynamics of fish locomotion is modeled using a three-dimensional (3D) computational fluid dynamics simulation of a thin undulatory plate. The rectangular plate model mimics the waveform of carangiform swimming by dividing the model into thirds along the axial flow direction with each section moving in a synchronized fashion. The Strouhal number (St) is a dimensionless parameter that is a function of oscillation frequency, fin tip amplitude, and flow velocity. Fish are found to naturally swim within a limited range of St that result in high propulsive efficiency. In this study, parameters of flow velocity, tail angular frequency, and amplitude of fin displacement were varied to investigate the thrust production and efficiency of the thin plate fin model. The results of this study show that this fish model achieves maximum propulsive efficiencies within the range of $0.3 \leq St \leq 0.5$ and that there is a dependence of the thrust production and efficiency on the St similar to the fish locomotion upon which it is based.

Keywords: fish, undulatory swimming, hydrodynamics, CFD, computational fluid dynamics, carangiform locomotion

I. INTRODUCTION

Vehicles such as submarines and airships combat gravity in a different way than an airplane or a rocket. Instead of creating an aerodynamic lift or exhaust thrust, the submarine's and airship's size allows for enough displacement of the respective fluid they move within to create a large enough buoyant force to counteract gravity. Since these neutrally buoyant craft do not need complex systems to generate lift, the main purpose of any propulsion system on board is to

^{a)} Author to whom correspondence should be addressed. Electronic mail: ntaluzek@gmail.com.

^{b)} This research was performed by Nicholas Taluzek during the Research Experience for Undergraduates program hosted by the Department of Aerospace Engineering at Texas A&M University.

^{c)} Dr. Sharath Girimaji served as the Faculty Advisor to Nicholas Taluzek during this research.

maneuver the craft at a constant altitude. Current propeller based propulsion systems can be very inefficient as they push a lot of the surrounding fluid in ways that do not generate thrust in the desired direction, creating wakes full of wasted energy that isn't being used to propel the craft. These systems are also unidirectional, being that a propeller can only create a force in one direction at a time unless the entirety of its exhaust is pivoted. While these systems do meet our current needs, we might be able to find a better propulsion solution within the nature that surrounds us.

Marine animals such as fish, whales, and dolphins are neutrally buoyant within their water home and employ a wave form motion in their swimming to propel themselves forward. Fish locomotion is still simplified down to Newton's law being that the fish exerts a force on the surrounding water which in turn acts on the fish's body. Using their musculature, they oscillate their bodies to generate an undulation motion that travels along the length of the body¹. As these waves propagate to the tail end of their body, their amplitude increases². This wave form motion generates vorticity that sheds at the end of the tail. There are different types of fish locomotion, depending on the shape motion of the body and the use of additional fins other than the caudal (tail) fin. The swimming motion that is focused on within this study is carangiform locomotion, where most of the wave amplitude is concentrated near the end of the body and the caudal fin³.

The dimensionless parameter known as the Strouhal number (St) can be used to describe the kinematics of fish locomotion. St can be used to study vortex shedding at fish tails using the following equation,

$$St = \frac{fA}{U} \quad (1)$$

where f is the frequency of vortex shedding, A is the characteristic length, and U is the surrounding fluid flow velocity. In the case of fish locomotion, f is related to the rate at which their tails oscillate from peak to peak, A is the distance from the tail tip at peak positions, and U is the relative speed of the fish to the oncoming water flow (See Figure 1). The results of this research will focus on the effect of the St parameter in fish locomotion.

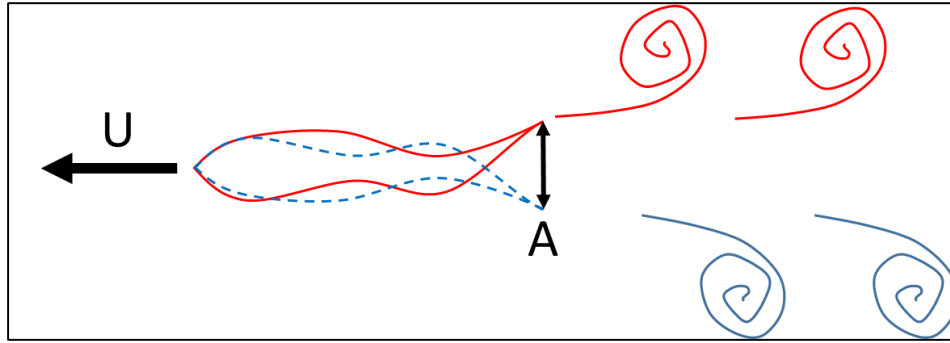


FIG. 1 – Shedding vortices from fish locomotion

Some studies suggest that fish and other marine animals can have propulsive efficiencies as high as 90%⁴. Creating mechanical systems with efficiencies this high would be a vast improvement to current technology and result in many benefits including increased travel durations, lighter fuel payloads, and more sustainable transportation. Fish are also very agile creatures that can turn directions in a much smaller space than the current craft, and the multidirectional propulsion that their bodies are able to perform is a key part of this. This study is one step forward in the development of a mechanical propulsion system to implement undulatory motion. Fish use biological structures of bone and muscle tissue to travel, and while duplicating their form might be possible and yield the high efficiencies we want, this would come with extra costs concerning the complexity of the machinery. The best design for our purposes would find the balance between performance and intricacy. This study looks at a 3-section thin plate that moves in a wave form mimicking carangiform locomotion. The simplified 3D computational fluid dynamics (CFD) model used in this research acts as a proof of concept that even simple systems can develop thrust, and that taking inspiration from nature's swimming animals might lead to future propulsion technologies.

II. METHODOLOGY

All preparation and simulation work for the computational fluid dynamics performed in this study was completed by using the commercial ANSYS Workbench Platform (Version 15.0) software. The DesignModeler was used to construct the geometry, Meshing to develop the grid, Fluent solver to run the simulations, and CFD-Post to create qualitative images and videos of the results.

A. Geometry

The chosen design for the fin model in this study is a thin flat plate because of the feasibility of constructing the fin for use in experimentation. An accompanying experimental study of the same fish locomotion was performed concurrently with this computational work during the summer of 2014. The final dimensions of the fin model were 0.15 m along the x-axis, 0.10 m along the y-axis, and 0.001 m thick along the z-axis. The fin was located such that the leading face of the rectangular box was centered at the coordinate system origin. See Figure 2 for dimensions of the fin. The domain of the simulation is cuboidal. The face of the domain set as the inlet is at the plane $(-0.5, 0, 0)$, and the length of the domain is 3.65 m . The cross section of the domain is 0.3 m by 0.3 m , centered at $y = 0, z = 0$. This domain was made as an enclosure within the DesignModeler which removed the enclosed fin body from the domain, allowing the fin geometry to be treated as a moving wall inside the fluid.

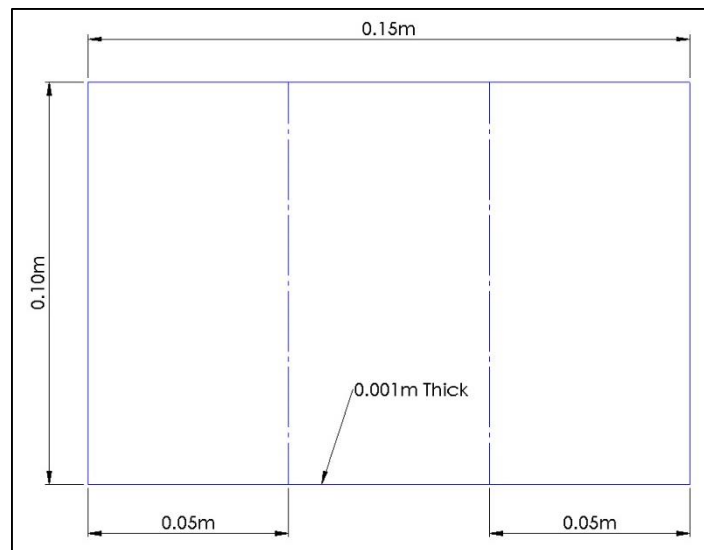


FIG. 2 – Dimensions of the fin model

B. Mesh

Across the face of the fin body the mesh was set to be finer than the surrounding domain, with the elements being only 0.005 m . The mesh was constructed with a total of 121,662 unstructured tetrahedral elements, making 23,294 nodes. See Figure 3 for images of the mesh fluid domain.

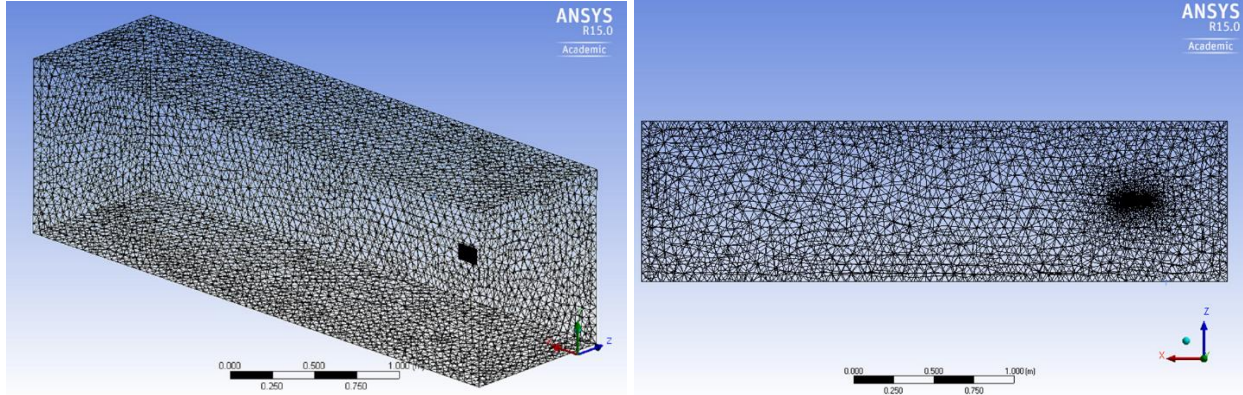


FIG. 3 – Isotropic view of mesh (Left) and Top down cross section view of mesh at midplane of fin (Right). Flow moves in the positive x-direction entering from the right most face

a. Dynamic Mesh

In order to create the desired fin movement, the Fluent solver’s software allows for setting up a dynamic mesh. In these simulations rather than having a fin object that is moving in the fluid, it is the mesh at the fin wall boundaries that is deforming into the shape of the undulating fin. Fluent allows the user to write a subroutine in C programming language called a User Defined Function (UDF) to perform operations that are not standard with the software. The Fluent UDF functionality also includes its own library containing macros and functions specific to the solver. To create the desired movement of the fin model, the `DEFINE_GRID_MOTION` macro is used. This macro allows each node within the mesh to be updated to a new coordinate after each time step. See Appendix A for the UDF code.

The motion we chose to have our fin perform is a three-section wave form intended to mimic the undulatory motion of carangiform locomotion. The fin model is evenly divided into three sections, each 0.05 m long. The first section does not move, as the body of a fish does not move much within the waveform. The second section then oscillates according to the sinusoidal function $\Theta_1 = A_1 \sin(\omega_1 t)$, where Θ_1 is the angle of the second section with respect to the first, A_1 is the angle magnitude for the section to move through from negative A to positive A, ω_1 is the angular frequency, and t is the simulation time. The last section of the fin oscillates as a whole section with respect to the joint between the first and second sections, but also pivots at its joint with the second plate to facilitate the carangiform waveform. This third section oscillates independently according to $\Theta_2 = A_2 \sin(\omega_2 t + \phi)$, where Θ_2 is now the angle of the third section with respect to the second and Φ is the phase difference between the second and third portions. The phase difference is critical in order to

have the waveform of this simplified plate model mimic that of fish undulation. Within this study, the phase difference was introduced at $t=T/4$, where T is the time period of oscillation constantly set at 2π . With each time step of the simulation a new relative angle is calculated for each section of the fin. As the UDF cycles through each node of the mesh to be updated, the distance from the node to the appropriate reference location (either the connection between the first and second section, or between the second and third section) is calculated, and then trigonometry is used with the new angle to calculate the new x and z coordinate for that node (there is no change in y locations for any part of the fin).

C. Simulation Settings

The Fluent software in this study is a computational fluid dynamics solver that uses the Navier-Stokes equations along with numerical methods to calculate values such as pressure, velocity, and vorticity at each element of the mesh. The simulations were solved with the pressure-based and transient state solver. The entire domain fluid is set as Fluent's default liquid water, with a viscosity of $1.003 \frac{g}{m \cdot s}$ and density of $998.2 \frac{kg}{m^3}$. The leading face of the domain is set as a free-stream inlet, the velocity of which is adjusted for each test case. The side boundaries and the back face of the domain are each set as pressure outlets, with the free-stream flow in the same axial direction as the inlet flow and a zero gauge pressure. The section of the domain distinguished as the fin is set as a wall with no-slip condition. See Table 1 for details about the dynamic mesh settings, these settings are what control how smooth the fin mesh shape is moved in each time step. Every simulation runs for 1000 steps, with a time step size of 0.01 seconds and a maximum of 50 iterations per time step. Residuals for the continuity, x -, y -, and z -momentum have values of 1×10^{-6} . The reference values for calculating the resulting drag and moment coefficients used for this study are set as the Area = $0.015 m^2$ and Length = $0.15 m$. The Pressure-Velocity Coupling setting SIMPLE is used, with least squares cell based gradient, second order pressure and second order upwind momentum spatial discretization. The transient formulation is first order implicit.

TABLE 1 – Settings for Dynamic Meshing within Fluent solver

Smoothing Mesh Method Settings	
Spring Constant Factor	1
Laplace Node Relaxation	1
Convergence Tolerance	0.001
Number of Iterations	30
Remeshing Method Settings	
Minimum Length Scale (m)	0.00246
Maximum Length Scale (m)	0.143164
Maximum Cell Skewness	0.944745
Maximum Face Skewness	0.9
Size Remesh Interval	5

III. RESULTS

Three sets of CFD simulations of the fin model were completed for this study, each set changed one of the variables used in calculating the St while the other two were held constant. The angular frequencies of the fin ranged from 1 rad/s to 30 rad/s, the inlet velocity from 0.02 m/s to 0.3 m/s, and the angles for both the 2nd and 3rd plate were tested from 0 degrees to 25 degrees individually while the other section was set at 10 degrees. These tested values for inlet velocity and angular frequency were chosen as suitable sets under which a small fish would be swimming⁵. Each set allowed for the model to be tested under a range of St numbers that previous work had shown to be the range under which fish naturally swim⁷.

A. Quantitative Data

The Fluent solver in each simulation calculated the pressure and velocity at each node on the face of the fin geometry. These values are then used to provide the drag and moment coefficients for the fin at each time-step of the simulation. An example of the CFD monitors for the drag and moment coefficients can be seen in Figure 4 and 5, respectively.

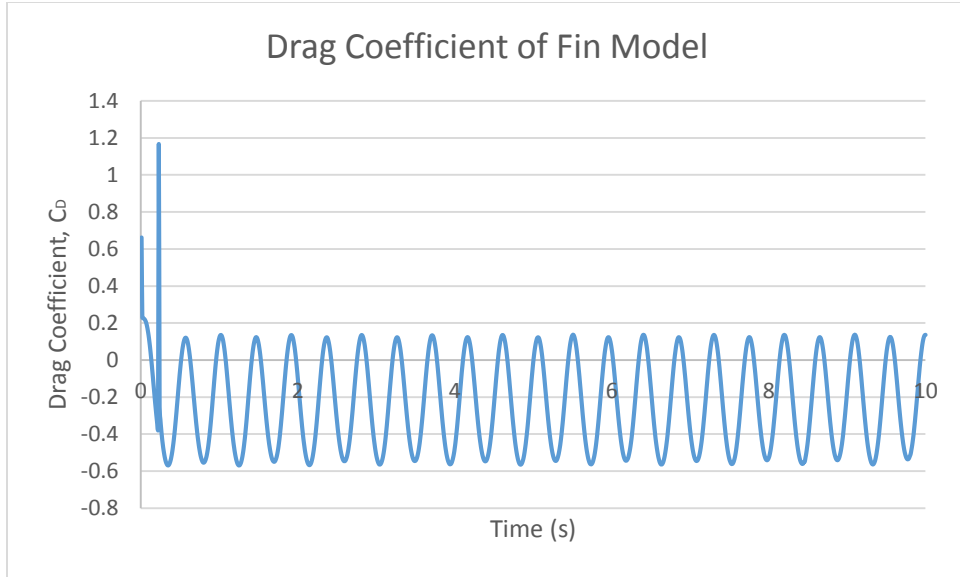


FIG. 4 – C_D plot for simulation with $f = 6 \text{ rad/s}$, $U = 0.1 \text{ m/s}$, $\max \Theta_1 = \Theta_2 = 10 \text{ degrees}$

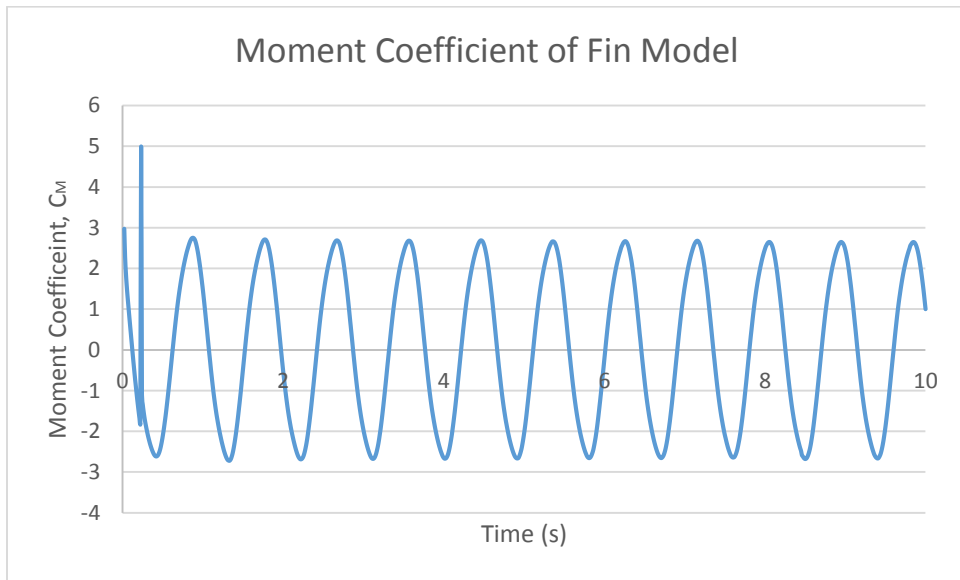


FIG. 5 – C_M plot for simulation with $f = 6 \text{ rad/s}$, $U = 0.1 \text{ m/s}$, $\max \Theta_1 = \Theta_2 = 10 \text{ degrees}$

The peak that is seen in each plot occurs at $t = \frac{T}{4}$, and this occurs because of the way the UDF was programmed. At $t=0$ the fin starts as a flat plate parallel to the free stream, and in order to create the phase difference between the 2nd and 3rd plate oscillations they both move together until $t = \frac{T}{4}$. At this time instant, the UDF code begins to implement the desired phase difference of $\frac{\pi}{2}$. Even though this changes the position of the third plate abruptly by a very minute angle, it

does seem to create a disturbance in the calculation at that time. So, the simulation data only after $t = \frac{T}{3}$ is used in the calculations.

The drag coefficient of the fin is indicative of the force it experiences along the x-direction. As can be seen in Figure 4, the drag coefficient has both positive and negative values. The positive drag values account for the force that push the fin in the direction of the flow, but the negative drag indicates a force acting against the flow. These negative drag coefficient values are the thrust coefficient values we are interested in. The simulations where the mean value of the drag coefficients is less than zero indicates that the fin model did produce a net positive thrust and if not for the constraints of the simulation, would propel itself against the flow of water. The calculation of the time average thrust coefficient for each simulation was done using the following equation 2,

$$C_T = \frac{\sum -c_D \times \Delta t}{nT} \quad (2)$$

where c_D is the drag coefficient provided in Fluent's results, Δt is the time step for the simulation, n is the number of periods to take the average across, and T is the period time⁶. Plots of the time average thrust coefficient with respect to the changing variable for each of the three sets of calculations can be seen in Figures 6, 7, and 8.

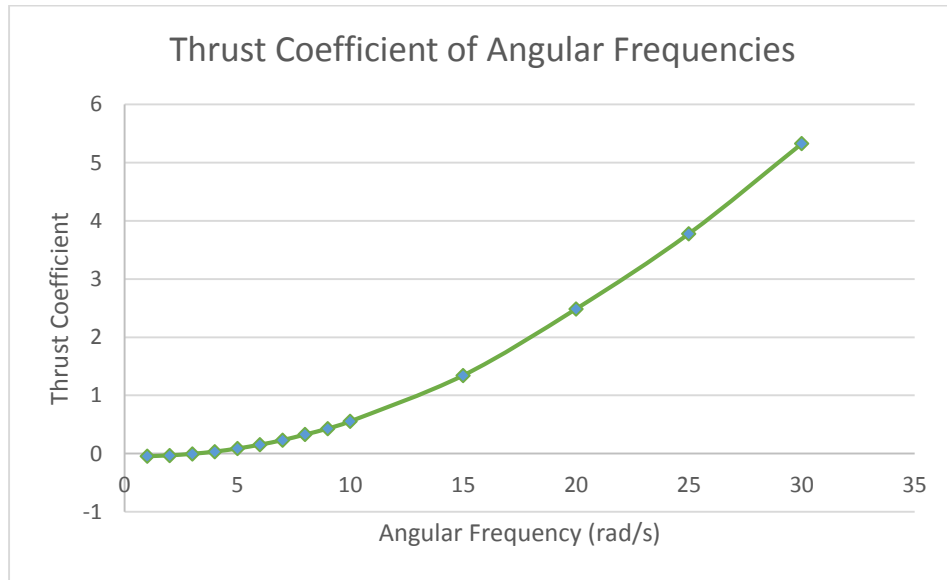


FIG. 6

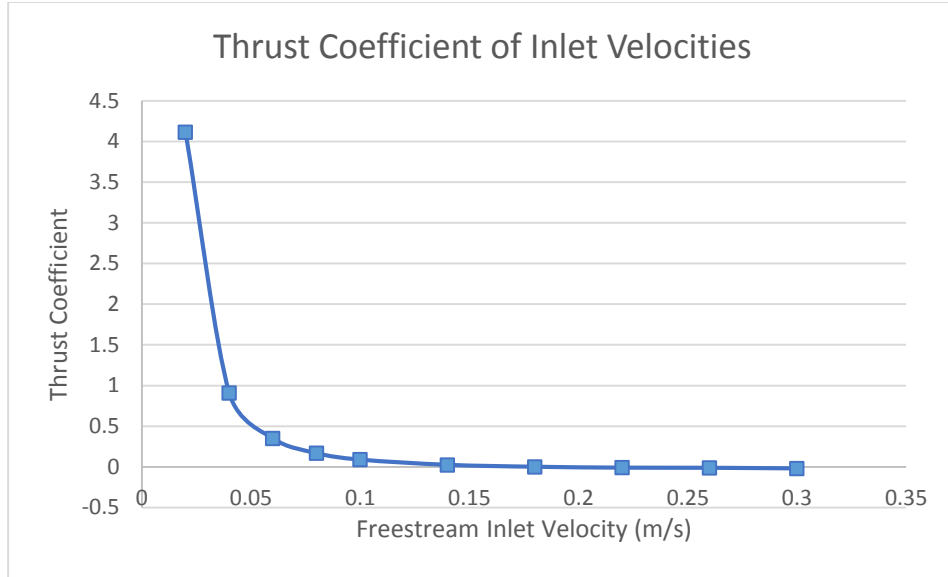


FIG. 7

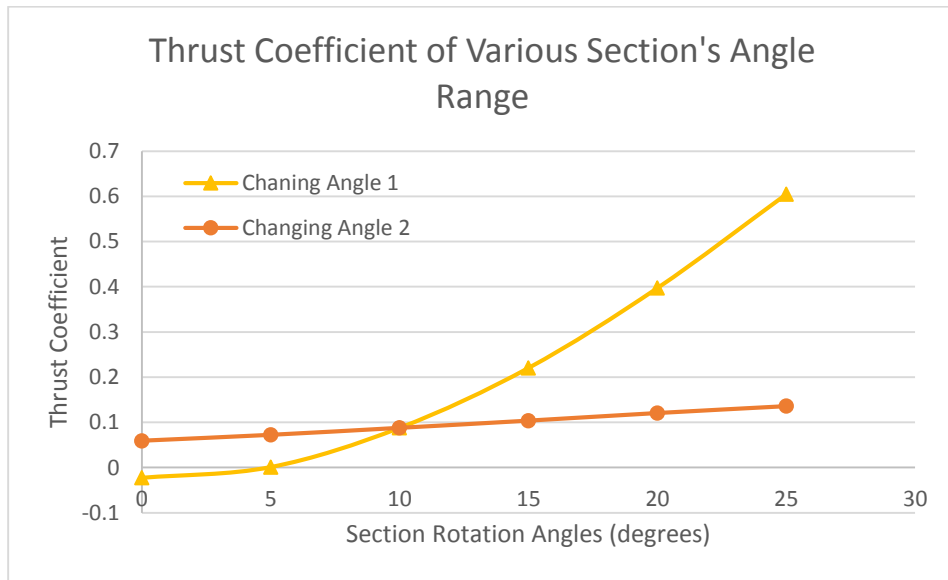


FIG. 8

The propulsive efficiency for the fin model was calculated using the following equation 3,

$$\eta = \frac{\text{Power In}}{\text{Power Out}} = \frac{C_T \times U}{\sum c_M \times \Delta t \times L \times \omega} \quad (3)$$

where U is the free stream inlet velocity, c_M is the moment coefficient of the fin provided in Fluent's results, L is the length of the fin body, and ω is the angular speed of the fin⁶. Due to the complex nature of the fin model, with two sections oscillating separately the true value of the fin's propulsive efficiency is unknown. The Fluent solver requires the input of a moment center

coordinate about which the moment calculation is done due to the pressure acting at each node of the fin body. Unable to correctly identify the appropriate coordinate location for the fin's moment center, all simulations were performed with it located at the coordinate system origin. This is at the center of the leading face side of the fin model. The calculation for the angular speed of the fin model was then done to be $\omega = (2\dot{\theta}_1 + \dot{\theta}_2)/3$, where $\dot{\theta}_1$ and $\dot{\theta}_2$ are the angular velocities at each time step for the second and third plate sections, respectively. This makes for a rough approximation of the angular velocity about the provided moment center coordinate. While the calculated values for the fin efficiency are not exact, they still allow for an approximate comparison for the efficiencies relative between each simulation test scenario. Plots of the propulsive efficiency with respect to the changing variable for each of the three sets of calculations can be seen in Figures 9, 10, and 11.

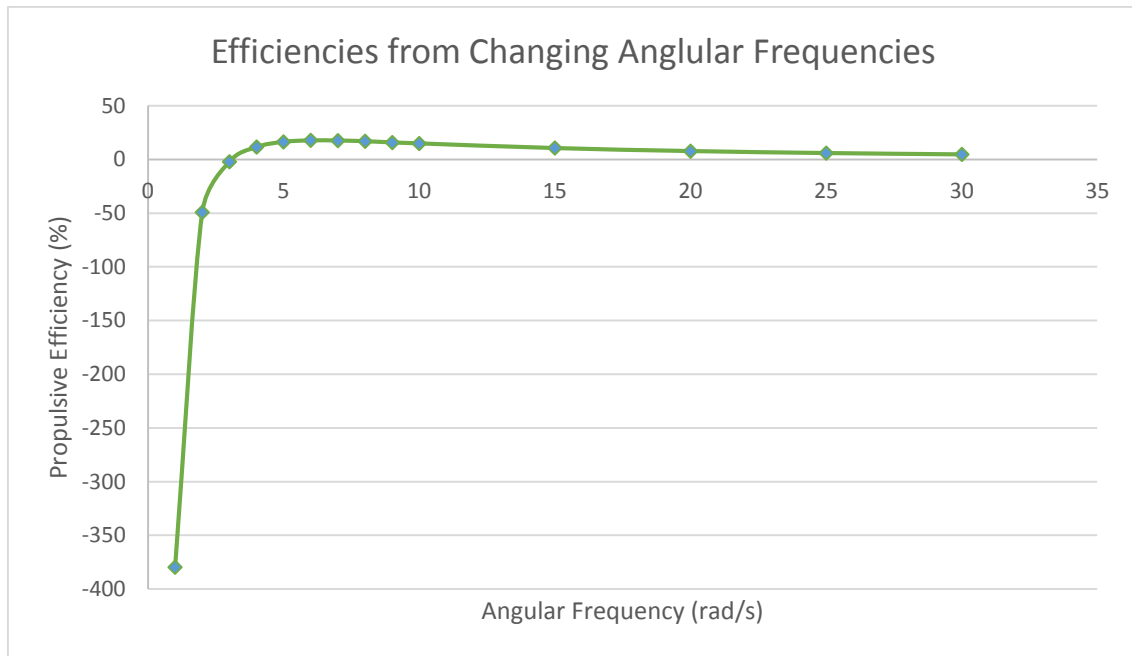


FIG. 9

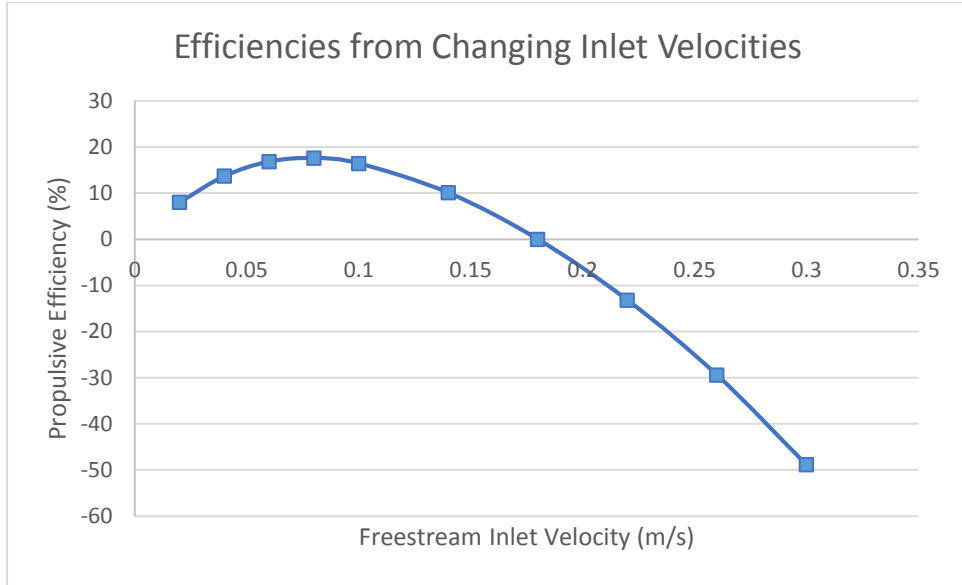


FIG. 10

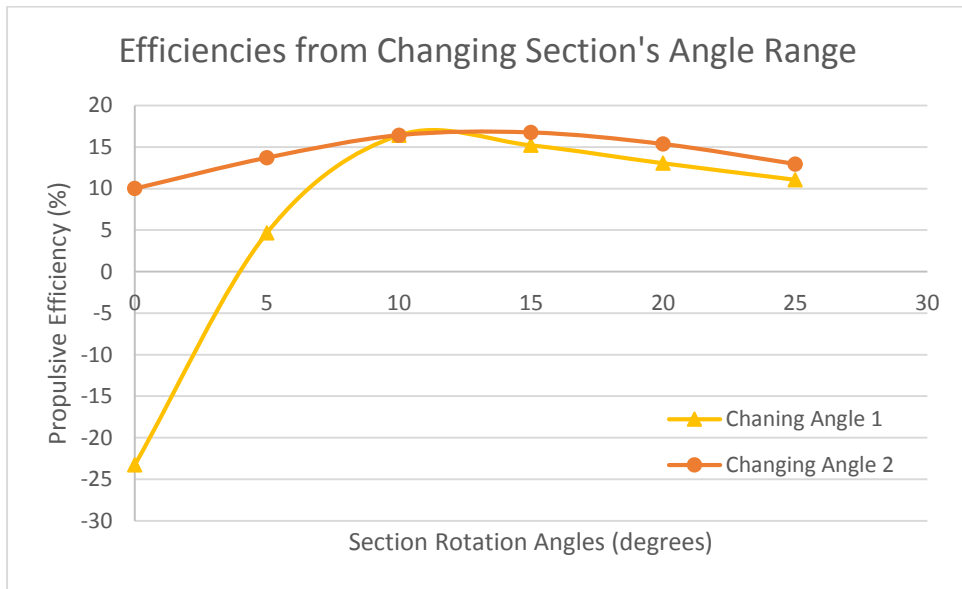


FIG. 11

B. Qualitative Visualizations

In addition to calculating the drag and moment coefficients, the ANSYS software suite also allows for the calculation of flow variables such as velocity, pressure, and vorticity at each element location throughout the simulation. The formation of vortices is of particular interest to this research, because it is the interaction between the vortices and the fish body that creates the propulsive forces. Data sets for each time step of the simulation with information about the vorticity were used within the CFD-Post software. Animations were made from these data sets to

visualize the vortices moving past the tail end to allow for qualitative analysis of the interaction, see Figure 12 for a series of images taken from these animations. The rainbow colored scale denotes the frequency of rotation, in Hz (s^{-1}), at a particular region within the water domain.

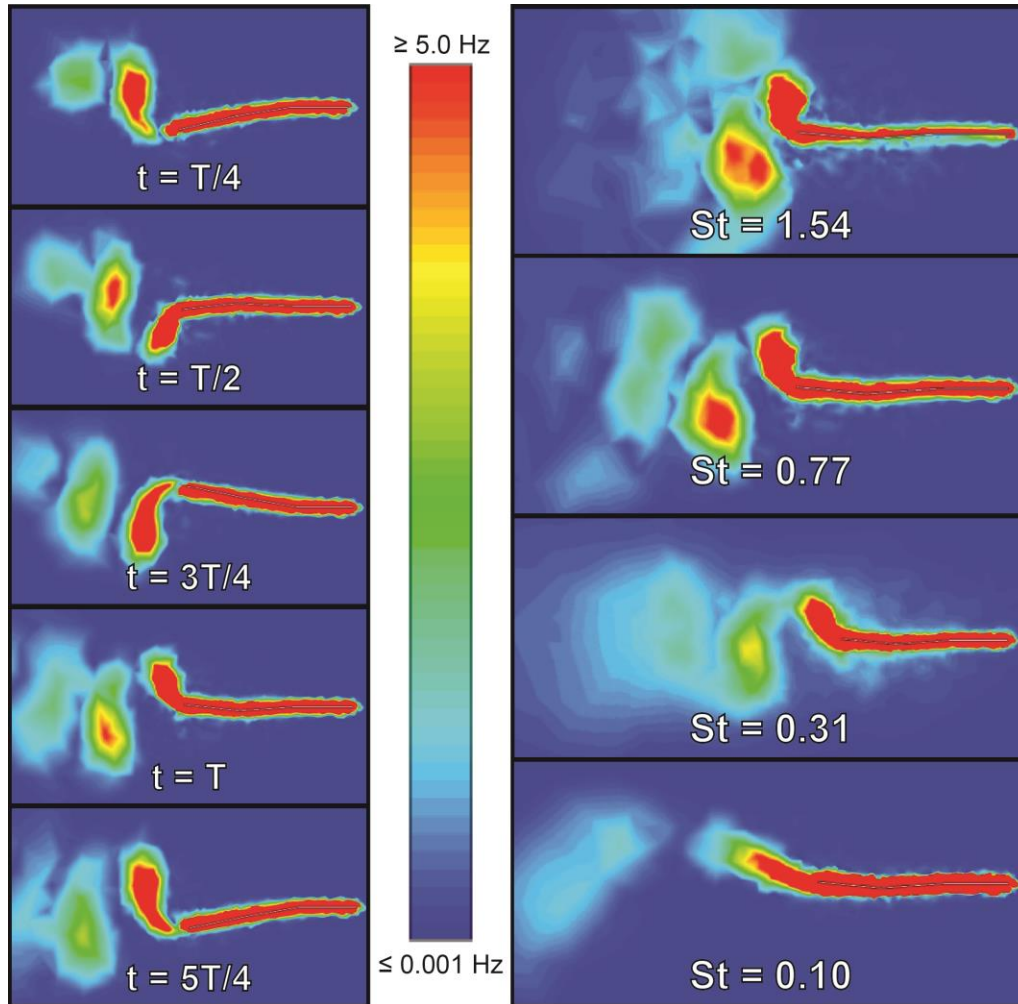


FIG. 12 – Top down vorticity contour plots of fluid at midplane of fin model. 12.a. – Images at different time periods with $St = 0.38$ (Left), 12.b. – Images at $t=T$ with various St values (Right)

IV. DISCUSSION

Each simulation within the three sets had one variable changed in order to have a collection of results across many St numbers. Figures 13 and 14 show the values of the thrust coefficient and relative propulsive efficiency of the fin model with respect to the St for the appropriate simulation settings that each data point was calculated from. The efficiencies are given relative to the highest value calculated, with $\eta = 0.1778$ being considered as its maximum possible propulsive efficiency and all other values set relative to that.

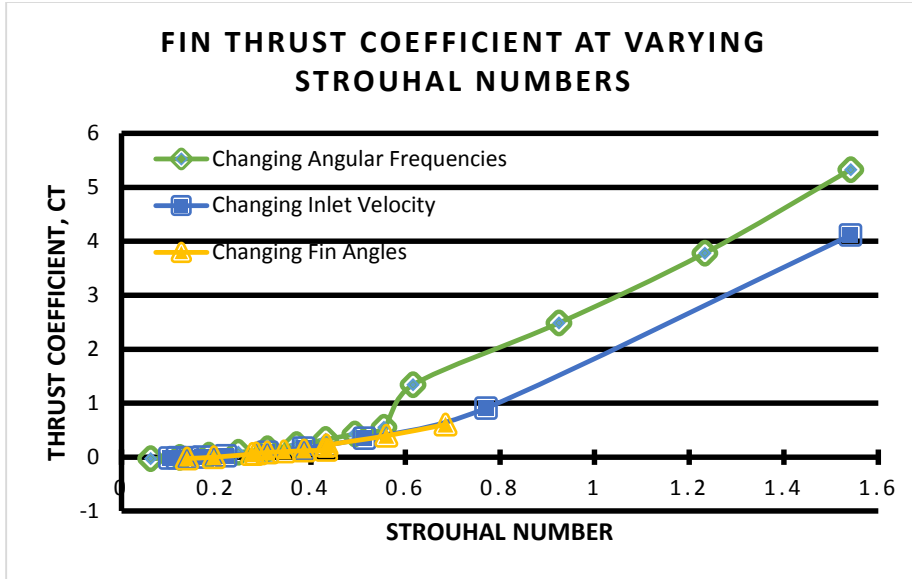


FIG. 13

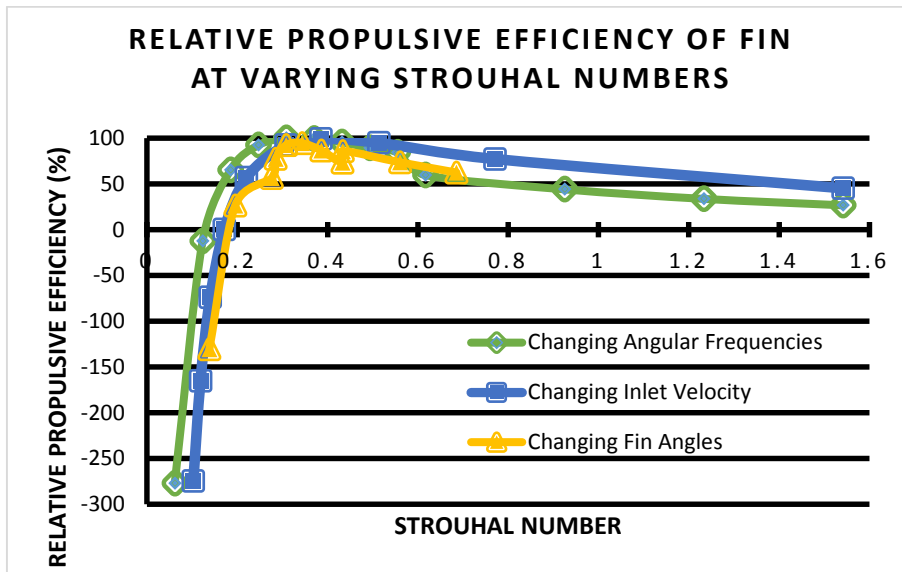


FIG. 14

It can be seen in Figure 13 that there is a clear correlation between the St and the thrust production. The higher the St , the more thrust produced. The environment in which a lot of thrust is produced is the one where the ratio between the frequency of the oscillations and the flow velocity is large. Under these conditions, vortices do not form properly behind the fin and a large region of water is disturbed behind it. From Figure 12.b., for $St = 1.54$, there are no cleanly defined regions of vorticity as opposed to $St = 0.77$.

Some of the simulations resulted in a negative thrust coefficient and efficiency. Within these simulations, all having $St < 0.2$, the fin did not produce enough thrust to act against the pressure drag and shear drag forces. The mean values of the drag coefficient across these simulations were positive. Negative efficiencies are indicative that the fin would not have propelled itself forward, being that work was put in to have the fin oscillate but no thrust was produced.

The most important conclusion that can be drawn from these results is the St range that yields the highest efficiency. This can be seen in Figure 14 that the optimal St for this fin model is $0.3 < St < 0.5$. Within this range there are well defined regions of vorticity behind the fin, as can be seen in Figure 12.b. High values of St create large amounts of thrust, but quickly lose efficiency as the water pushed backwards by a brute force as opposed to the lower St scenarios that allow the water to move smoothly and fully form each vortex as it moves past the fin. It can be seen how individual vortices form over time in the flow visualization of Figure 12.a. Our results agree with previous research into animals that use oscillating patterns during locomotion, which has shown the St range which fish and other animals naturally move within is between 0.25 and 0.4^{7,8,9}.

Each set of simulations closely followed the same behavior, and all three did peak in efficiency at the same St range. There is a notable difference between the thrust and efficiency values for the changing angular frequencies and inlet velocity simulation sets, but no conclusions about this can currently be drawn from this limited set of data points. The set with changing fin section angles was not tested at high St but is expected to show the same trends as the other simulation sets. The two subsets of angle simulations had some differences between efficiencies at similar St settings, and this can be attributed to the complexity of the fluid flow around different fin body movements. These subsets faced different magnitudes between pressure drag and shear drag depending on which section was set to oscillate at small or large angles.

A. Error Analysis

A handful of challenges in using CFD made room for error in these simulations. As mentioned previously, the largest discrepancy in these results comes from Fluent's use of a moment center coordinate. After running test simulations it was seen that changing the position of the moment center in the simulations could change the resulting efficiency by ± 0.06 . However, the relative efficiency plots with different moment centers did not change, so the

qualitative understanding of the St number's relation to thrust and efficiency can still be considered valid. The calculations were performed to only include the oscillation periods after $T/3$, however it is unclear how the simulation time before this might affect the resulting values later in the simulation. Due to limited computing time, simulations were only ran for a time up to 10 seconds. Each calculation carried out for the thrust and efficiency values used as many oscillation periods as possible. However, in the simulation sets of changing angular frequency some simulations were able to complete more than others. In testing the calculations, it appeared that a larger number of oscillation periods that were able to be completed in the simulation, and thus used in the calculations, resulted in slightly higher efficiency values for that simulation test case. The simulations with lower inlet velocities also never reached a state where the fluid domain behind the fin would have a uniform trail of vortices behind the fin. The tolerance settings for the continuity, x-, y- and z-momentum were all set to $1E-06$ within Fluent but the simulations were only set to perform 50 iterations for each 0.1 second time step, and the residuals never reached values smaller than $1E-04$.

B. Future Work

Just as this work expanded upon previous research that only involved a single sectioned oscillating fin model, there is still much to be done to study fish locomotion by means of computational fluid dynamics. If this study of a three-section plate is to be continued then the correct moment center needs to be calculated in order to yield accurate efficiency values. The moment center issue was not discovered until the end of the research period and due to time limitations it was not corrected for. Under current understanding of the Fluent solver, only one location can be set as the moment center for the entire simulation and having multiple points of rotation (such as the two pivot points for the second and third section) may lead to further challenges. One possible solution to allow for proper moment calculations would be creating the fin model with individual objects for each fin segment, separated by a very small gap space, and allowing Fluent to calculate the moments from each segments respective pivot coordinate. Alternatively, another CFD solver might be considered for use that allows for more functionality in calculating the work input into the system.

Additional tests with this model should be performed to develop a stronger understanding of the hydrodynamics. A small sampling of tests were completed that changed the angles each

section of the fin moved through, and while these tests generally displayed the same efficiency behavior related to the St , there were some nuances to the data that need to be looked at further. All of the simulations done in this study had the fluid set with a constant free stream velocity in order to have results to compare to another concurrently operating water tunnel experiment, but further work should be done to understand the dynamics of the fin in standing fluid. Many fish live within bodies of water that often have little to no fluid movement, such as small ponds, and seeing the fin model under these conditions could lead to greater insight about the propulsive forces involved in fish locomotion.

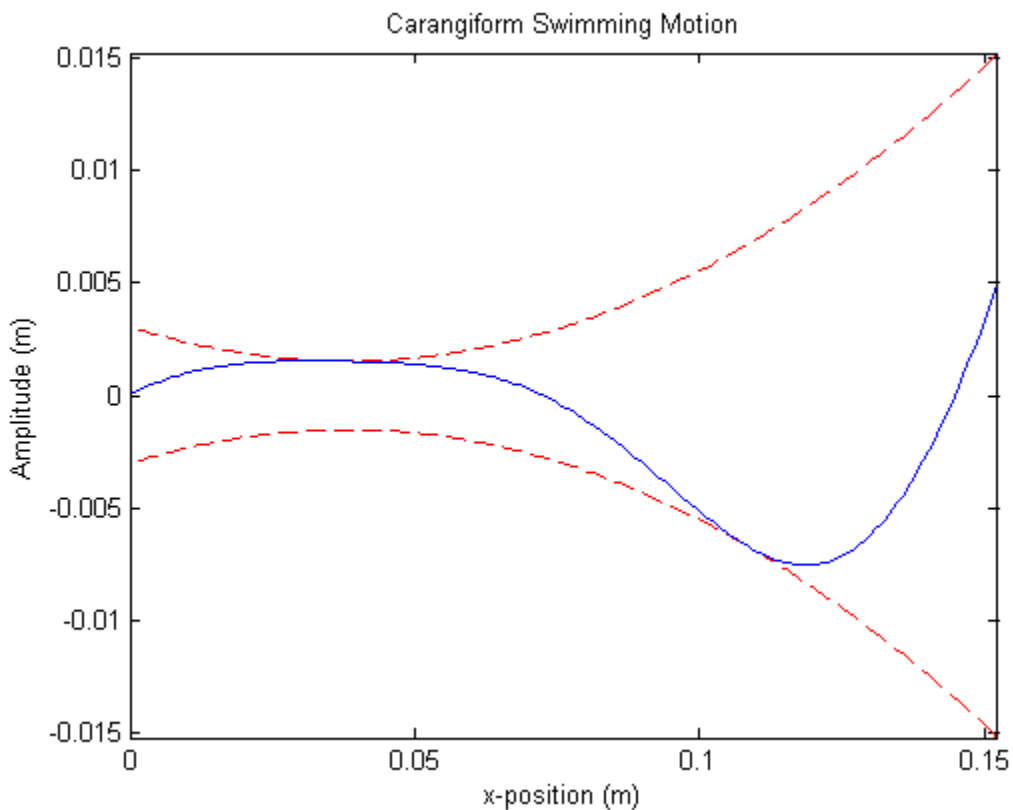


FIG. 15 – Plot of carangiform characterization equation³, $h(x,t)=(a_0+a_1x+a_2x^2)\sin(kx-\omega t)$

The fin model used for this study was chosen for its simplicity to reproduce for real-world experimentation and to establish a baseline understanding of what efficiencies to expect from a basic fin model. The movements of this fin model are very limited being that it is comprised of only three sections, the first of which was held stationary. To yield efficiencies for a propulsion system to replace modern propeller engines used in submarines and airships, it is likely that the fin design will need to increase in complexity. A higher number of divisions in the plate would

allow for a motion more closely resembling the carangiform wave pattern. In Figure 15 the blue line indicates the centerline of the fish body, and the dashed red lines are the upper and lower displacement limits at the respective x-positions along the body. But any future work to create CFD modelling of fish locomotion should also be done to find a model design that is balanced between yielding high propulsive efficiency while still being mechanically simple. This research is not intended to copy fish locomotion, but rather take inspiration from it in order to design an efficient propulsion system for our own purposes.

V. CONCLUSION

This study was completed to understand the hydrodynamics of undulatory fish locomotion, and by changing select variables the 3D three-section thin plate model used to represent a fish was tested under a range of Strouhal numbers to see the resulting performance. In this study thirty five CFD simulations were completed, split into three groups that varied either angular frequency, inlet free stream velocity, or fin section angle ranges. Results of the simulations provided information about the drag and moment coefficients for the fish model, which were then used to calculate the thrust produced and efficiency of the tail. Due to time limitations and difficulties in using the Fluent CFD solver, the efficiency values we calculated are not quantitatively valid but can be compared to each other qualitatively between the different test cases. The optimal propulsive efficiencies were observed within the Strouhal number range of 0.3 to 0.5, which closely matches previous research. The expected behavior of the Strouhal number affecting the thrust coefficient was also seen, that an increase in St leads to an increase in thrust produced but at the cost of efficiency. In addition to the numerical data, video files of vorticity contour plots were processed from the simulations to qualitatively view the vortex separation at the end of the tail model.

Taking inspiration from nature to help develop new technologies is an excellent way to expedite the invention process, being that evolution has already taken many years to lead to some highly efficient systems. The fin model in this study is a rough approximation to the motions that the complex fish musculature can perform, but it is one step toward developing new propulsion innovations. The roughly calculated efficiencies for this study's fin model peaked at just about 18%, which is not high enough yet to compete with current propeller propulsion used in submarines and airships. Creating a mechanical system with efficiencies as high as the fish they

are modeled after would be a significant technological advancement and with further research into modeling fish locomotion, that type of system may be created soon.

VI. ACKNOWLEDGEMENTS

This work has been made possible thanks to the support from my research advisor, Dr. Sharath Girimaji. The knowledge and skills that I gained during this Research Experience for Undergraduates program is invaluable and will be of great use to me as I graduate and move into my career. Another big thanks to the graduate students who I worked with, Zach Harris and Divya Sri Praturi, whose help was always appreciated. Additional support for this work came from fellow undergraduate students that shared in all of my success and failures along the way, Jeremy Diaz and John Rangel.

This material is based upon work supported by the National Science Foundation under Grant No. 1157070. Any opinions, findings, and conclusions or recommendations expressed in this material are those of the authors and do not necessarily reflect the views of the National Science Foundation.

APPENDIX A: Fin Oscillation User-Defined Function

```
#include"udf.h"
#include"math.h"

/* This is the udf written for the "double flapper" geometry. The overall length of the
flapper is 0.15m, width is 0.1m, thickness is 0.01m.
The leading face of the rectangular prism is centered at the coordinate system origin
(0,0,0).
The udf assigns two angular velocities to two parts of the fin. For the 2014 REU
simulations, the fin sections were divided at 0.05m and 0.10m.
*/

int main() /* main() is included because Fluent v15.0 presented issues for us when
compiling the UDF if it was not present. */
{
    return 0;
}

DEFINE_GRID_MOTION(oscillate_theta_final,domain,dt,time,dtime)
/* Fluent UDF macro used to control the movement of the mesh. In our case, we assigned
the fin wall object as a user-defined Dynamic Mesh. This macro must be compiled by Fluent
first before using. */
{
    Thread *tf = DT_THREAD(dt);
    face_t f;
    Node *v;
    /*Declaring variables used throughout the UDF*/
    real NV_VEC(origin1),NV_VEC(origin2), NV_VEC(rvec), NV_VEC(rvec2);
    real NV_VEC(rvec0), NV_VEC(dx0), NV_VEC(new_vec), NV_VEC(new_vec0);
    int n;
    int i;
    real pi=3.1415926;
    real j, angle1, angle2, freq1, freq2, L, theta1, theta2;

    SET_DEFORMING_THREAD_FLAG(THREAD_T0(tf));

    /* These are the values used to change the fin movement.
    angle1 is the maximum angle for the 2nd section of the fin relative to the
    horizontal.
    Example: If angle1 = 30*pi/180; then the 2nd section of the fin will move
    in a range from -30 degrees to +30 degrees from the horizontal x-axis.
    angle2 is the maximum angle for the 3rd section of the fin relative to the
    horizontal.
    freq1 and freq2 are the angular frequency for the 2nd and 3rd section of the fin,
    respectively. */
    angle1 = 30*pi/180;
    angle2 = 15*pi/180;
    freq1 = 2;
    freq2 = 2;

    /* theta1 and theta2 are calculating the change in the angle for the newest
    iteration time step.
    For theta2 there is a phase difference set to start at 1/4 of the period because
    the fin starts as a flat plate, and this gives it time to reach the appropriate angles we
    want for the simulations.
    The recorded values for drag, lift, and moment coefficients for time < T/4 are
    discarded from calculations. */
    theta1 = angle1*(sin(time*freq1)-sin((time-dtime)*freq1));
```

```

j=time/(2*pi/freq1);
if (j < 0.25){
theta2 = 0;
}
else {
theta2 = angle2*(sin(time*freq2-pi/2)-sin((time-dtime)*freq2-pi/2));
}

/* setting origin coordinates and code to update origin2 (the point between the 2nd
and 3rd sections of the fin) for each time step */
NV_D(origin1,=,0.05,0.0,0.0);
NV_D(origin2,=,0.10,0.0,0.0);

new_vec0[0]=0.05*cos(angle1*sin(time*freq1));
new_vec0[2]=0.05*sin(angle1*sin(time*freq1));
new_vec0[1]=origin2[1];
NV_V(new_vec0, +=, origin1);
NV_V(origin2, =, new_vec0);

/* looping over all the nodes on the threads */
begin_f_loop(f,tf)
{
f_node_loop(f,tf,n)
{
v=F_NODE(f,tf,n); /* gets the address of the current node */

if(NODE_X(v)>0.05 && NODE_POS_NEED_UPDATE(v)) /* node beyond 1st section of
fin and needs update */
{
NV_VV(rvec,=,NODE_COORD(v),-,origin1);
L=sqrt(rvec[0]*rvec[0]+rvec[2]*rvec[2]);

new_vec[0]=L*cos(theta1+atan(rvec[2]/rvec[0]));
new_vec[2]=L*sin(theta1+atan(rvec[2]/rvec[0]));
new_vec[1]=NODE_COORD(v)[1];
NV_V(new_vec, +=, origin1);
NV_V(NODE_COORD(v), =, new_vec);
if (NODE_X(v)<=origin2[0]) /* nodes before the x-position of origin2.
ie. the 2nd portion of the fin */
{
NODE_POS_UPDATED(v);
}
else /* remaining 3rd section of the fin gets moved another time for a second
rotation, but this time around origin2 */
{
NV_VV(rvec2,=,NODE_COORD(v),-,origin2);
L=sqrt(rvec2[0]*rvec2[0]+rvec2[2]*rvec2[2]);
new_vec[0]=L*cos((theta2)+atan(rvec2[2]/rvec2[0]));
new_vec[2]=L*sin((theta2)+atan(rvec2[2]/rvec2[0]));
new_vec[1]=NODE_COORD(v)[1];
NV_V(new_vec, +=, origin2);
NV_V(NODE_COORD(v), =, new_vec);
NODE_POS_UPDATED(v);
}
}
}
}
}

```

REFERENCES

- [1] Sfakiotakis, Michael. (1999). Review of fish swimming modes for aquatic locomotion. *IEEE Journal of Oceanic Engineering*. 24(2), 237 – 252. doi: 10.1109/48.757275
- [2] Videler, J., Hess, F. (1983). Fast Continuous Swimming of Two Pelagic Predators, Saithe (Pollachius Virens) and Mackerel (Scomber Scombrus): a Kinematic Analysis. *J Exp Biol* 109, 209-228.
- [3] Borazjani, I., Sotiropoulos, F. (2008). Numerical investigation of the hydrodynamics of carangiform swimming in the transitional and inertial flow regimes. *J Exp Biol* 211, 1541-1558. 10.1242/jeb.015644
- [4] Muller, U.K., Van den Huevel, B.L.E., Stamhuis, E.J., and Videler, J.J. (1997). Fish foot prints: Morphology and energetics of the wake behind continuously swimming mullet (Chelon Labrosus Risso). *J Exp Biol* 200, 2893-2906.
- [5] Bainbridge, Richard. (1957). The Speed of Swimming Fish as Related to Size and to the Frequency and Amplitude of the Tail Beat. *J Exp Biol* 35, 109-133.
- [6] Anderson, J. M.; Streitlien, K.; Barrett, D.S.; Triantafyllou, M.S. (1998). Oscillating foils of high propulsive efficiency. *Journal of Fluid Mechanics*. 360, 41-72.
- [7] Eloy, C. (2012) Optimal Strouhal number for swimming animals. *Journal of Fluids and Structures*. 30 205-218. ISSN 0889-9746. dx.doi.org/10.1016/j.jfluidstructs.2012.02.008
- [8] Taylor, G., Nudds, R., Thomas, A. (2003) Flying and swimming animals cruise at a Strouhal number tuned for high power efficiency. *Nature*. 425, 707-711. doi:10.1038/nature02000
- [9] Triantafyllou, M.S., Grosenbaugh, M.A. (1993). Optimal Thrust Development in Oscillating Foils with Application to Fish Propulsion. *Journal of Fluids and Structures*. 7(2) 205-224. ISSN 0889-9746. <http://dx.doi.org/10.1006/jfls.1993.1012>